44th AIAA Aerospace Sciences Meeting and Exhibit, 9-12 January 2006, Reno, NV

# Measurements of wall shear stress of an offset attaching planar jet with co-flow

Nan Gao and Dan Ewing

*Dept. of Mech. Eng., McMaster University, Hamilton, Ontario, Canada, L8S 4L7*

Jonathan W. Naughton

*Dept. of Mech. Eng., University of Wyoming, Laramie, Wyoming, 82071*

**The distributions of the wall shear stress and the Stanton number for an offset attaching planar jet with a Reynolds number of 43000 and a co-flowing jet was measured experimentally using thin oil film interferometry and a heated thin foil. The flow fields, static wall pressure and the fluctuating wall pressure were also measured to examine the effect of the velocity ratio had on the development of the jets. It was found that the lower jet was entrained into the upper jet for low velocity ratios and the two jets seem to develop parallel to each other for larger velocity ratios. The change in the skin friction was found to be associated with the mean flow and the static wall pressure, while the change in the heat transfer seemed more closely related to the turbulence in the shear layer.**

## Nomenclature

| | |
|---|---|
| $H_c$ | Height of the splitter plate between two jets, m . |
| $H_s$ | Offset distance from lower edge of the upper jet to the wall, m . |
| $H_j$ | Height of the upper jet, m . |
| $H_l$ | Height of the lower jet, m . |
| $C_f$ | Skin friction coefficient, $2\tau_w/\rho U_a^2$ . |
| $C_P$ | Static wall pressure coefficient, $2(P - P_\infty)/\rho U_a^2$ . |
| $C_{p'}$ | Fluctuating wall pressure coefficient, $2p'/\rho U_a^2$ . |
| $c_p$ | Specific heat of air, $J/KgK$ . |
| $h$ | Convective heat transfer coefficient, $W/m^2K$. |
| $P$ | Static wall pressure, $Pa$ . |
| $p'$ | RMS value of the fluctuating wall pressure, $Pa$ . |
| $q_{conv}$ | Convective heat flux to the flow over the foil, $W/m^2$. |
| $q_{elec}$ | Total Joulean heating, $W/m^2$. |
| $q_{rad}$ | Radiation heat loss from the foil, $W/m^2$. |
| $Re$ | Reynolds number, $U_U H_j/\nu$. |
| $St$ | Stanton number, $h/\rho c_p U_U$. |
| $T_j$ | Jet temperature, $K$. |
| $T_w$ | Foil temperature, $K$. |
| $U_L$ | Flow rate averaged velocity of the lower jet at the exit, m/s . |
| $U_U$ | Flow rate averaged velocity of the upper jet at the exit, m/s . |
| $u'$ | RMS value of the horizontal component of the velocity fluctuations, m/s . |
| $\langle uv \rangle$ | Reynolds stress, $m^2/s^2$ . |
| $v'$ | RMS value of the vertical component of the velocity fluctuations, m/s . |
| $X_r$ | Attachment length, m . |

$x$ Spatial coordinate in the streamwise direction, m .
$y$ Spatial coordinate in the vertical direction, m .
$y_{+1/2}$ Outer half jet width of the upper jet, m .
$z$ Spatial coordinate in the cross-stream direction, m .
$\nu$ Kinematic viscosity of air, $m^2/s$.
$\rho$ Density of air, $kg/m^3$.
$\tau_w$ Skin friction, $Pa$.

# I. Introduction

Offset attaching planar jets can be found in a number of cooling applications. Previous investigations have characterized the development of the Reynolds averaged flow field in turbulent offset planar jet analytically,[19] experimentally,[13,18] and numerically using RANS models[14] primarily for cases when the distance of the lower edge of the jet from the wall was greater than the jet height. The heat transfer from the wall to the flow was also characterized in these cases.[15] In these flows, a planar jet, initially traveling parallel to a wall, curves toward the adjacent wall as it develops downstream and eventually attaches to the wall due to the Coanda effect at a downstream position that depends on the initial distance of the jet to the wall.[13] Part of the flow travels upstream forming a recirculation flow region and the reminder travels downstream and recovers to a two dimensional wall jet. The interaction of the flow with the wall produces a maximum in the static wall pressure and convective heat transfer rate.[13,15] In these offset jets, the reattachment length ($X_r$) increases with offset distance, but the ratio of these distance $X_r/H_s$ decreases.

Tanaka et al.[20–22] studied the development of radial attaching jets discharged from a cylindrical nozzle when air was blown or sucked though a gap in the corner of the recirculation region. The initial direction of the additional flow was perpendicular to the direction of the attaching jet. A suction flow shifted the location of the reattachment upstream and increased the maximum in the static pressure, while a blowing flow had the opposite effect. This effect was more pronounced for higher added flow rates or for attaching jets with smaller offset distances. Forliti and Strykowski[5] found that the turbulence of the shear layer formed by a backward facing step increased when suction was applied in the recirculating region of the flow . Gao et al.[8] and Gao and Ewing[6] recently examined the development of an offset attaching jet with a second low speed co-flowing jet issuing between the main jet and the wall. They found that the low speed jet was entrained into the main jet before the main jet attached to the wall, but the attaching process of the main jet could be modified by the second jet. The measurements in this case were performed for a limited range of velocity ratios typical of those used in the blown film cooling applications. It was not clear whether the lower jet remained attached to the wall in the near field in these cases. Until now, there has not been experimental investigations of the heat transfer or the skin friction for offset planar jets with a co-flowing jet.

The objective of this investigation is to characterize the effect that a coflowing jet had on offset planar jets for a wide range of velocity ratios. The development of the jets were characterized using measurements of the flow field with hot-wire anemometry, measurements of the wall pressure and measurements of the skin friction that are useful in characterizing the flow near the wall. The convective heat transfer from a heated wall to the jet were also measured. The experimental facility and methodology used in this investigation will be discussed first. The results will then be presented and discussed.

# II. Experimental Methodology

The development of the jets was examined using the two jets in the facility shown in Fig. 1. Both jets in this facility exited long channels designed so that flows at the exit would be nearly fully developed. The air flow to the facility was supplied from a 10 HP blower. The flow was split into five hoses that led to a 122cm by 72.4cm by 45.7cm settling chamber attached to the upper channel, and three hoses that led to a 81.3cm by 40.6cm by 22.9cm settling chamber attached to the lower channel. The hose connections included gate valves that were used here to adjust the flow to the jets. Both settling chambers included layers of foam and perforated plates to condition the flow. The width of both channels was 74.3cm. The height of the upper channel was 3.8cm so the ratio of the upper jet width to its height was 19.5, while the height of the lower jet was 1.8cm so the aspect ratio of this jet was 41. The lower edge of the upper jet was 3.8cm above the wall, so ratio of the offset distance of the jet to the jet height, $H_s/H_j$, was 1.

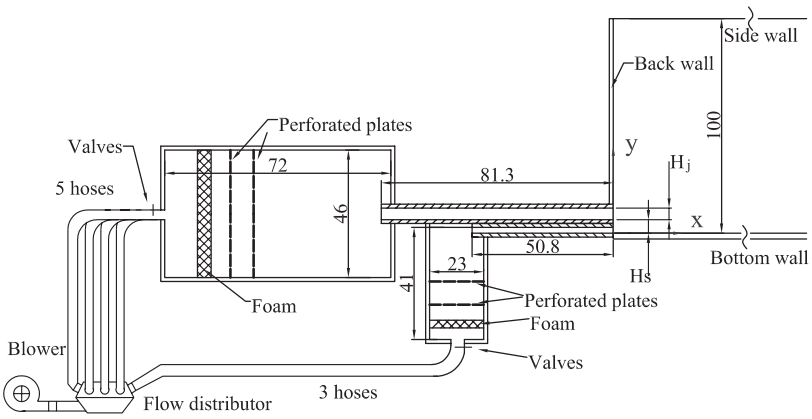


**Figure 1. Schematic of the dual attaching planar jet facility with an offset ratio $H_s/H_j = 1.0$.**

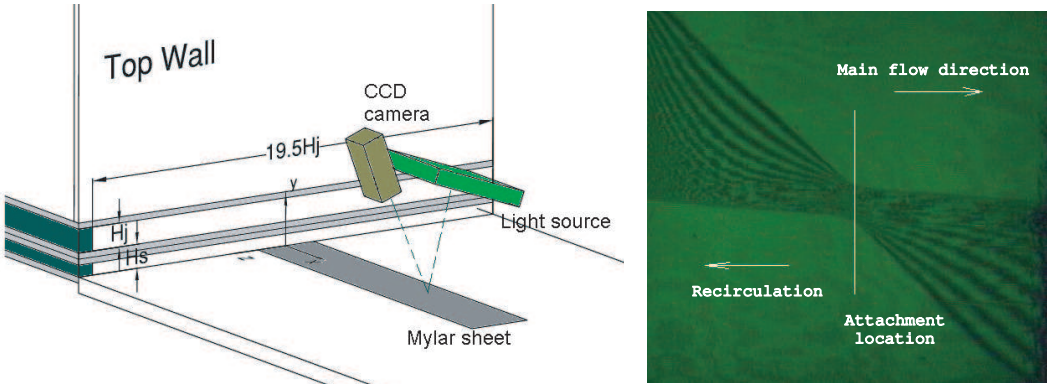


**Figure 2. Schematic of the oil-film interferometry and a typical fringe pattern near the attachment point.**

The flow exiting the channels develops over a 1.8m long plate that was mounted parallel to the channels. The vertical position of this plate can be adjusted using supporting screws to produced a planar wall jet. The flow was confined using a 80cm high back wall and two 100cm high and 180cm long side walls. The profiles measured along both channels outlet were uniform over the central region of the jet from $-6 \leq z/H_j \leq 6$, with variations in mean and rms velocity less than 2% and 5%, respectively. The effect of the side walls on the two dimensionality of the jets was also checked by measuring the boundary layer on the side walls as the flow evolved downstream. The thickness of these layers grew to approximately $7H_j$ at $x/H_j = 20$.

The development of the flow field in the offset jets was measured using a cross hot-wire probe and an in-house anemometry system. The measurements were performed using a probe with a wire diameter of $5\mu$m and length of 1.5mm. The hot-wire probe was calibrated using a jet exiting a contoured nozzle that had a uniform velocity profile. The resulting response curves were fit with four-order polynomials and the cross-wire was calibrated using a modified cosine technique.[10] The flow field was measured by moving the hot-wire probe on a computer controlled traverse that could be positioned with an accuracy better than 0.05mm. At each point, the output signal from the anemometry system was sampled using a 14-bit A/D board at a frequency of 4096Hz for a total time of 50 seconds. The uncertainties for mean velocity and rms velocity measurements due to sample size evaluated following the approach in Bruun[3] are less than 1% and 3%, 19 times out of 20, respectively. The ambient air temperature during the measurements was measured using a RTD temperature sensor with a resolution of $0.1^oC$. The temperature varied less than $\pm 1^oC$ in all cases and the effect of the temperature on the velocity measurements was compensated using the technique proposed by Beuther.[1]

The static pressure on the bottom wall was measured using a series of pressure taps mounted along the jet centerline. The pressure taps were located at $1 \leq x/H_j \leq 8$ at a spacing of $0.5H_j$, and $9 \leq x/H_j \leq 12$ at a spacing of $H_j$. The fluctuating pressure was measured using 16 Panasonic WM-60B microphones, that

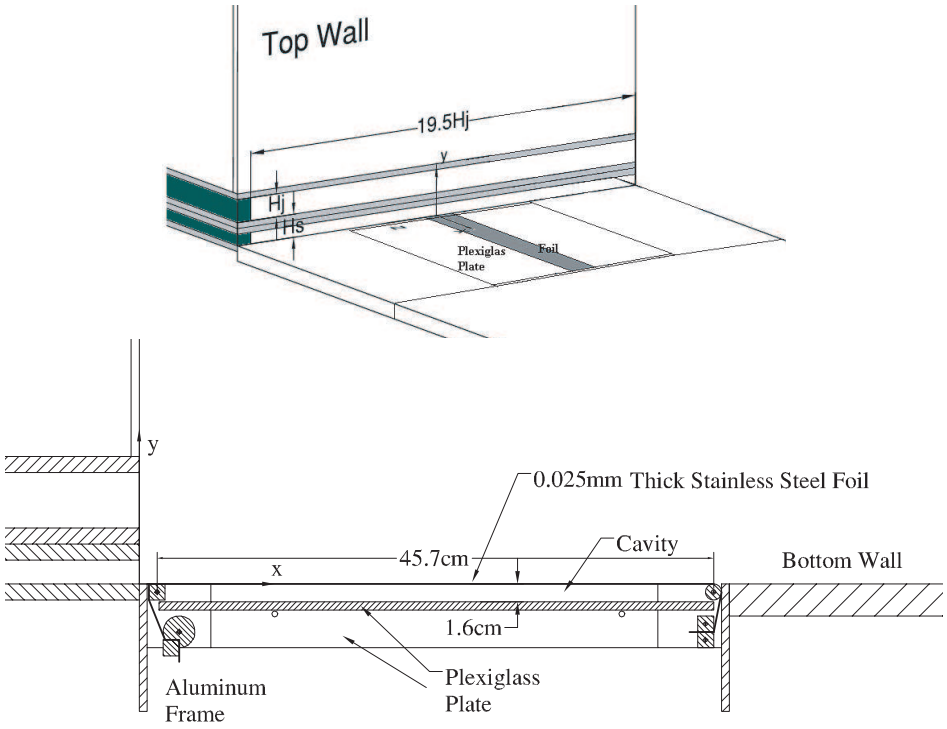


**Figure 3. Schematic of the heat transfer set up.**

have a flat response for 20Hz to 5000Hz. The microphones were mounted directly into blind cavities drilled from the bottom of the wall on a line 0.75 cm off the centerline of the jet. The cavities were located at $1 \leq x/H_j \leq 7$ at a spacing of $0.5H_j$, $8 \leq x/H_j \leq 10$ at a spacing of $H_j$, and $x/H_j = 12$ and 14. The microphones sense the flow through a 1mm-diameter, 5mm-long pinhole drilled through the wall to the top of the cavity. Measurements indicated that the lowest resonance frequency was approximately 2000Hz. The microphones were calibrated in situ using a piston phone at 1000Hz. The signals from microphone were simultaneously acquired with the 14-bit A/D board in 100 blocks of 4096 data points at a frequency of 4096Hz. The uncertainties for the static and fluctuating wall pressure due to the sample size were less 2% and 5%, respectively, 19 times out of 20.

The skin friction on the wall is measured using thin-oil-film interferometry technique. The background and development of this method is discussed in detail in Naughton and Sheplak.[16] In these measurements, the central part of the bottom wall is covered using a 91cm by 13cm thin Mylar film shown in Fig. 2. Dow Corning 200 Fluid with a nominal viscosity of 20cs is applied on the Mylar film. In most of the cases, oil was applied as a line approximately $45^o$ to the direction of the main flow. The oil film was illuminated using a mono chromatic lamp producing green light with a wave length of 546.1nm. The flow was then run at the desired condition and the resulting fringe patterns were acquired using a Pulnix TMC-7DSP CCD camera and a Matrox Meteor II frame grabber. The camera and light source were mounted on a traverse that can move to 9 locations in streamwise direction to cover the area of interest. After the experiment was started, the computer sent a trigger signal to the camera to take an image every 5 minutes, while the dynamic head of the jet at the center of the jet exit and the jet temperature were monitored using a pitot tube and a RTD sensor, respectively. The changes of the oil viscosity with the temperature were accounted for in this technique. Detailed description of this method can be found in Naughton *et al.*[17]

The convective heat transfer rate from the heated wall to the jet was measured using the facility shown in Fig. 3. The facility contained two plexi-glass plates mounted on an aluminum frame with a 45.6cm by 10cm gap between the plates. A 0.025mm thick stainless steel foil, that acted as the heat transfer surface, was mounted over this gap. A 1.6mm thick plexiglas plate was located under the foil to form a 1.6cm thick cavity below the foil to reduce the heat loss from the bottom of the foil. The foil was attached to adjustable aluminum mounts positioned below the surface, used to tension the foil after it was heated. The ends of the foil were clamped to the adjustable aluminum mounts using machined square aluminum bars. Heavy gauge

wires were used to connect these bars to a regulated DC power supply that could produce approximately 1500 $W/m^2$ of local electrical heating in the foil. The current through the foil was measured using a meter on the power supply, while the voltage drop across the foil itself was measured using a multi-meter.

The heat generated by the foil was transferred to the jet, lost by radiation from the foil, transferred to the air below the foil, or conducted through the foil. The radiation heat transfer from the foil, $q_{rad}$, was less than 7% of the local electrical heating. The heat transfer to the air below the foil was estimated by assuming the air was stratified in the cavity below the foil and the loss was estimated to be less than 1% of the local heating. Similarly, the lateral heat conduction in the foil based on the temperature gradients was less than 0.5% of the total electrical heating. These latter two losses were neglected but considered in the uncertainty analysis. Thus, the local heat transfer coefficient for the impinging jet was given by

$$h = \frac{q_{conv}}{T_w(x) - T_j} = \frac{q_{elec} - q_{rad}}{T_w(x) - T_j}, \tag{1}$$

where $T_w(x)$ was the local foil temperature and $T_j$ was the jet temperature measured using a thermocouple at the jet exit and a Fluke 52II thermometer. The top of the foil was coated with candle-soot black paint that was found to have an emissivity of $0.96 \pm 0.01$.[9] The local temperature distributions of the foil were measured using a FLIR THERMACAM SC3000 infrared camera located directly above the foil. The thermal camera was calibrated using an isothermal surface where the temperature was measured using a thermocouple. The total uncertainties of the measurement of $T_w - T_j$ is estimated to be less than $0.5^oC$ using the approach outlined by Coleman and Steele.[4] The heat transfer coefficient was reported in Stanton number, $St = h/\rho c_p U_U$, which is typical in the investigations of the reattaching flow.[23] The uncertainty of the Stanton number was estimated to be less than 7%, 19 times out of 20.

The measurements were performed here for cases where the upper jet velocity, $U_U$, was 18m/s corresponds to a Reynolds number of 43 000. The velocity of the lower jet from 0 to 14m/s that corresponds to velocity ratio of approximately 0 to 0.8. The Reynolds numbers in these cases were 0 to 16 300. The lower jet exit was blocked using tape in the case when the lower jet velocity was 0 to create an uniform boundary condition.

## III. Results and Discussions

The distributions of the mean velocity vectors, the corresponding streamlines, and the coefficients of the static pressure and skin friction for co-flowing jets with velocities of 0, $0.2U_U$, $0.4U_U$ and $0.6U_U$ are shown in Fig. 4. The results show that the upper jet alone curved and attached to the wall at $x/H_j \approx 4.6$ before recovering into a wall jet. The distribution of the skin friction indicates that a recirculation region was formed between the wall and the jet, as expected, causing a negative skin friction coefficient in the recirculation region with a minimum at $x/H_j \approx 4$, similar to the results from the backward facing step.[2,12] The skin friction increased to 0 at the reattachment location where the local static pressure gradient was approximately 0 and further increased to a maximum at $x/H_j \approx 8$ where the streamlines of the jet were approximately parallel to the wall. The skin friction gradually decreased downstream of this point similar to a planar wall jet as discussed in more detail below. The change in the static wall pressure was closely related to the change in the streamline curvature of the mean flow. The static wall pressure was initially below the atmospheric pressure and continued to decrease as the jet initially curved toward the wall reaching a minimum static pressure coefficient at $x/H_j \approx 3$ (or $x/X_r \approx 0.65$ similar to the backward facing step[11]). The static pressure then increased and reached a maximum slightly downstream of the attachment point where the curvature of the mean flow away from the wall was largest (again similar to other reattaching flows). The static pressure then decreased gradually to atmospheric pressure at $x/H_j \approx 8$, which coincides with the maximum skin friction.

When the lower jet velocity was $0.2U_U$, the lower jet separated from the wall near the jet exit due to the adverse pressure gradient along the wall as evidenced by the negative skin friction in this region. The jet was entrained into the upper jet and the merged jet attached to the wall at $x/H_j \approx 5.3$, further downstream of the reattachment point of the single offset jet. The negative skin friction before reattachment location was smaller than the single offset jet indicating the recirculating flow was less prominent in this jet. The curvature of the attaching jet with the co-flow was also more gradual than the offset jet without co-flow so the static wall pressure below the recirculating region and the reattachment region was also smaller.

The development of the jet appeared to change when the velocity of the lower jet was increased to $0.4U_U$. The lower jet appeared to curve away from the wall, but it was not entrained by the upper jet near the exit

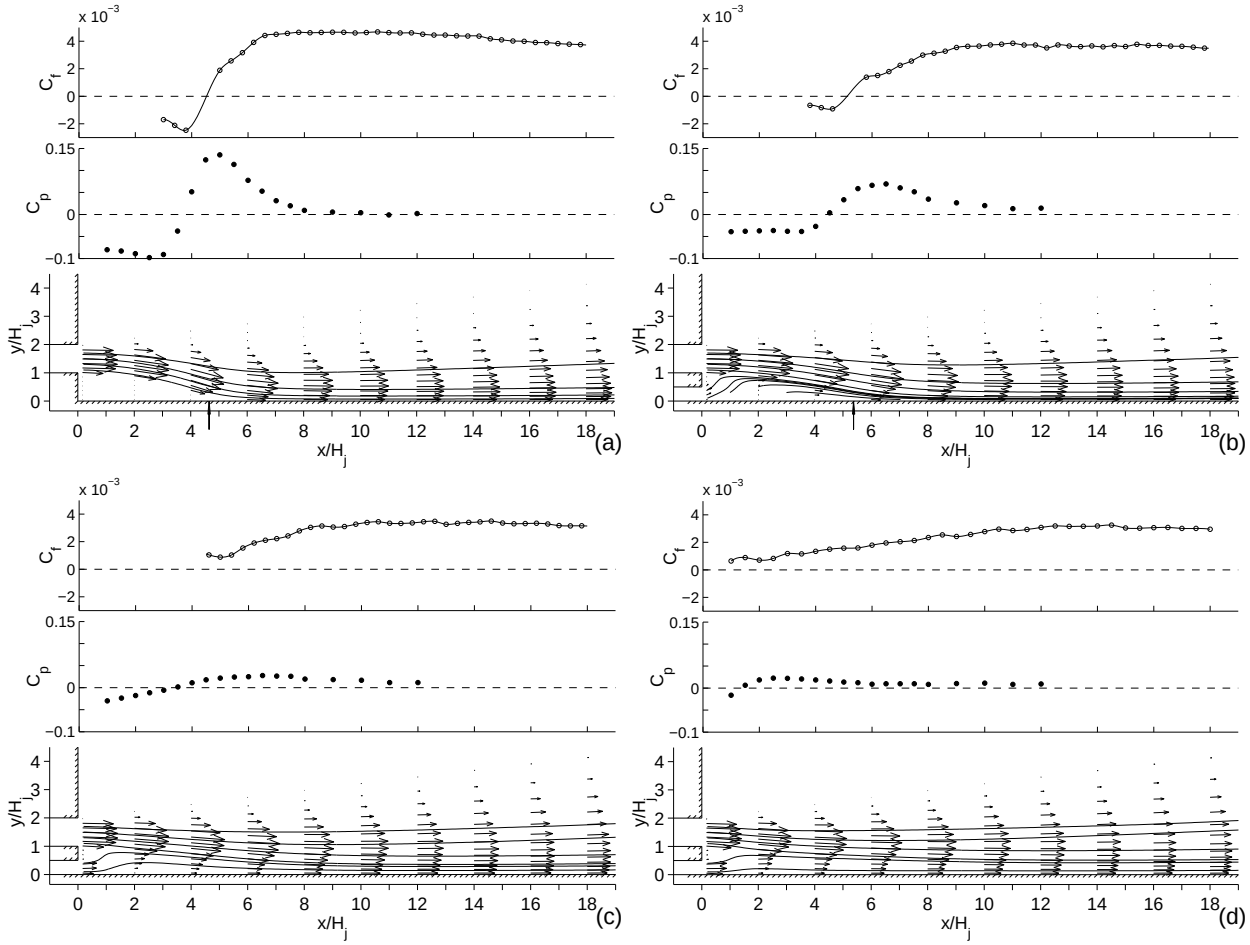


**Figure 4. Distributions of the skin friction coefficient, $C_f$, the static wall pressure coefficient, $C_P$, and the vectors and streamlines of the mean velocity for jets with velocity ratios of (a) 0, (b) 0.2, (c) 0.4 and (d) 0.6.**

as in the case of $U_L/U_U = 0.2$. Instead, the two jets seemed to develop parallel to the each other. Both jets then gradually curved toward the wall as the flow evolved downstream. The skin friction in the region $x/H_j \leq 4$ was small so it was not possible to measure it accurately. The visual observation of the oil film showed that the mean skin friction was positive indicating that the lower jet continued to develop along the wall and there was no separation at least in a mean flow sense. The negative pressure near the jet exit was higher than the pressure below the recirculating region for jet with $U_L/U_U = 0.2$. The maximum in the static wall pressure was much lower, however, because the streamline curvature associated with the jet attaching to the wall was smaller. The static wall pressure and the skin friction increased gradually as the upper jet approached the wall reaching maxima at $x/H_j \approx 7$ and $x/H_j \approx 10$, respectively.

The change in the skin friction was even more gradual when the velocity ratio was further increased to 0.6. In this case, the skin friction was clearly positive everywhere along the wall indicating that the lower jet did not separate from the wall, but there was still evidence of the lower jet being decelerated near the exit. The static pressure reached a local maximum near the jet exit $x/H_j \approx 2.5$ due to the local curvature behind the splitter plate that caused a deceleration of flow near the wall. The maximum skin friction did not occur until $x/H_j \approx 13$ indicating the increase in the shear stress was more gradual and driven by momentum transfer across the flow rather than the acceleration of the flow near the wall associated with the reattachment. When the velocity ratio was further increased to 0.8, similar trends were observed and the maximum skin friction occurred even further downstream at $x/H_j \approx 16$.

The effect of the velocity ratio on the development of the upper jet can also be characterized by the

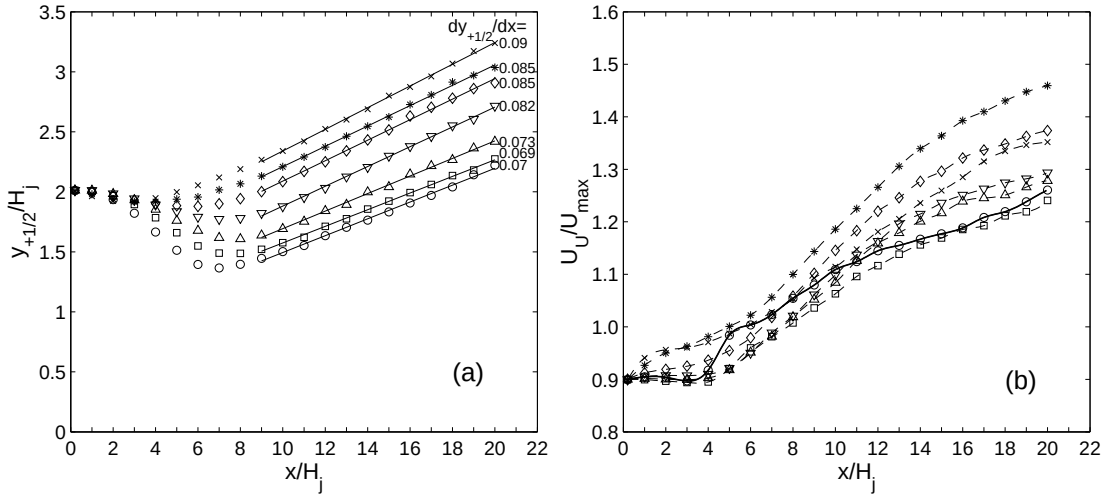


**Figure 5. The distributions of (a) the outer half jet width of the upper jet and the (b) the maximum local upper jet velocity for jets with velocity ratio $U_L/U_U = \circ$ 0, $\square$ 0.1, $\triangle$ 0.2, $\triangledown$ 0.3, $\Diamond$ 0.4, $*$ 0.6 and $\times$ 0.8.**

change in the outer half jet width and the decay of the maximum velocity of the upper jet shown in Fig. 5. The distributions of the outer jet half width and the maximum velocity indicate that the flow went through two changes when the velocity ratio was increased, one between $U_L/U_U \approx 0.2$ and 0.4 and a second between 0.6 and 0.8. All the jets initially curved toward the wall in the region $x/H_j \leq 5$. The length of this region was larger for the cases where the lower jet velocity was smaller. The maximum velocities in this region were approximately constant for jets with $U_L/U_U \leq 0.3$ before decreasing significantly when the jet attached to the wall, similar to the single offset jet. For larger velocity ratio, $U_L/U_U \geq 0.4$, where the lower jet appeared not to be entrained by the upper jet, the maximum velocity in the upper jet decayed gradually to $x/H_j \approx 6$ where the potential core of the upper jet ended. The upper jet velocity then decayed more rapidly. The half jet width of all the jets grew approximately linearly in the region $x/H_j \geq 9$. The growth rates of the outer half jet width, $dy_{+1/2}/dx$, for the jets with $U_L/U_U \leq 0.2$ were approximately 0.07, similar to the single offset jet, while the growth rate for jets with $U_L/U_U \geq 0.3$ were significantly higher at 0.08 to 0.09 more similar to the values observed in a free jet, suggesting that the development of the outer shear layer is not as affected by the interaction with the wall in these cases at least in the regions studied here. For the jets with velocity ratios less than 0.6, the maximum velocity in the upper jet decayed more rapidly than the jets with lower velocity ratios in the region $6 < x/H_j \leq 20$. The decay rate for the case with $U_L/U_U \approx 0.8$ was smaller than $U_L/U_U \approx 0.6$ indicating that there may be another transition between the velocity ratios of 0.6 and 0.8.

The distribution of the fluctuating velocities and Reynolds shear stress, $u'$, $v'$ and $\langle uv \rangle$ for jets with velocity ratios of 0, 0.2, 0.4 and 0.6 are shown in Fig. 6. The distributions of the fluctuating wall pressure and Stanton number are also shown in this figure. The Stanton number in the region $x/H_j \lesssim 7$, $7 \lesssim x/H_j \lesssim 15$ and $13 \lesssim x/H_j \lesssim 17$ were measured separately by placing the heat transfer surface at different downstream locations. Small difference in the bulk temperature of the jet resulted in some discrepancies in the Stanton number but there was generally good agreement in the measurements performed at different locations.

The changes in the Stanton number and the fluctuating wall pressure were similar in the regions where the upper jet interacted with the wall and were closely related to the turbulence near the wall. For the jets with $U_L/U_U \leq 0.2$ the shear layers developed on each side of the upper jet. The rms velocity of the inner shear layer increased as the flow evolved downstream and reached a maximum slightly upstream of the reattachment point. The turbulence from the inner shear layer soon decreased as the flow developed downstream, while turbulence in the outer shear layer became larger and dominated the outer part of the flow field. The fluctuating wall pressure and the Stanton number was small in the recirculation region and increased to a maximum near the reattachment location. The fluctuating wall pressure and the Stanton number both decreased gradually after the reattachment as the rms velocity of the inner shear layer decreased. The turbulence levels did not changed significantly when the velocity ratio was increased from 0 to 0.2.

When the velocity ratio was $U_L/U_U \approx 0.4$ or greater, there was a dramatic increased in $v'$ and $\langle uv \rangle$ in the inner shear layer of the outer jet. The Stanton number and the fluctuating wall pressure coefficient (based

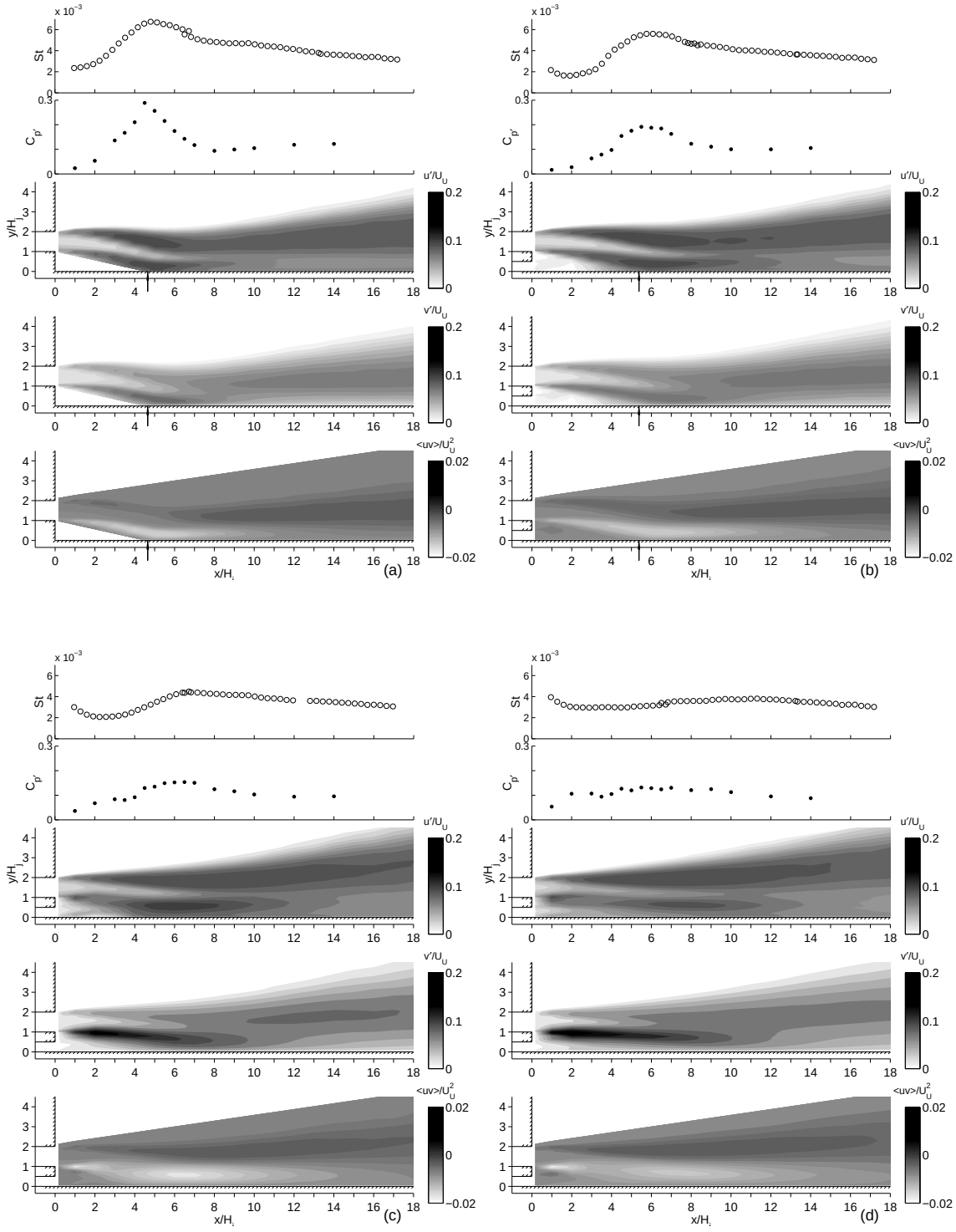


**Figure 6. Distributions of the Stanton number, $St$, fluctuating wall pressure, $C_{p'}$, fluctuating velocities, $u'/U_U$ and $v'/U_U$, and Reynolds shear stress, $\langle uv \rangle / U_U^2$, for jets with velocity ratios of (a) 0, (b) 0.2, (c) 0.4 and (d) 0.6.**

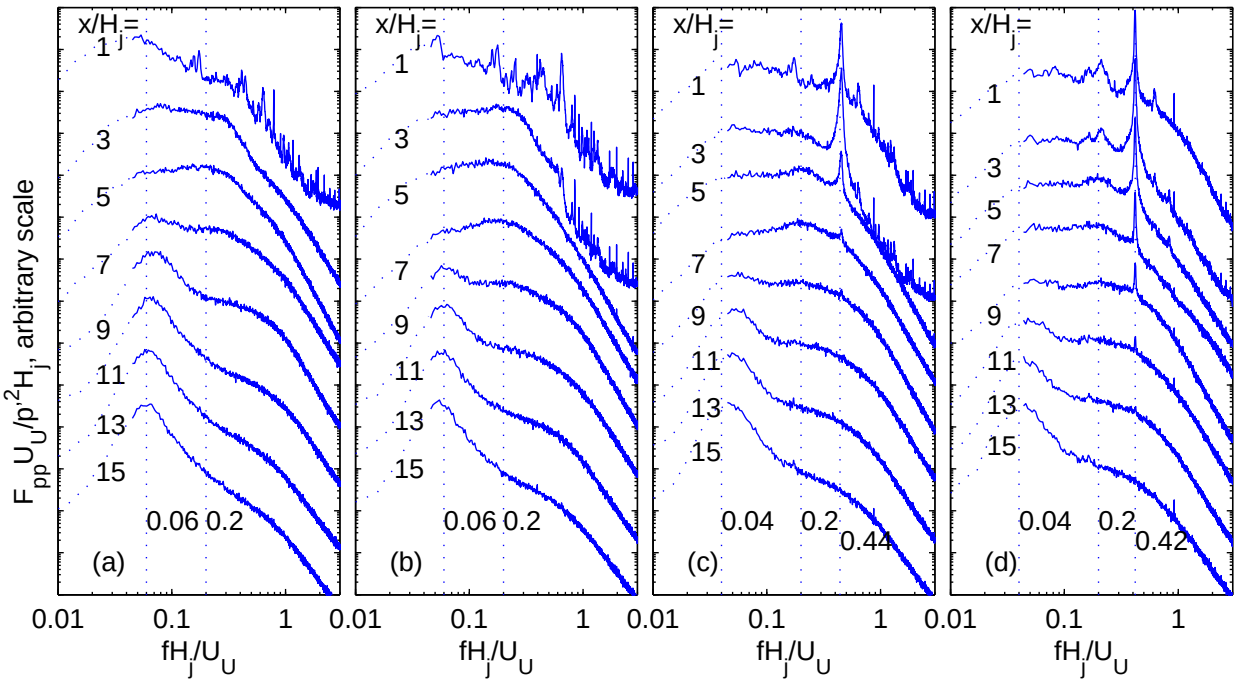


**Figure 7. The spectra of the fluctuating wall pressure for jets with velocity ratios of (a) 0, (b) 0.2, (c) 0.4 and (d) 0.6.**

on the upper jet velocity) near the jet exit increased as the lower jet velocity increased as expected. The maxima in the fluctuating wall pressure and Stanton number were smaller where the upper jet interacted with the wall than the cases with smaller velocity ratios despite the dramatic increase in the turbulence in the inner shear layer of the upper jet. This suggests the turbulent structures developed in this shear layer were attenuated as the shear layer initially interacted with the wall without causing a large increase in the heat transfer.

The spectra of the fluctuating wall pressure for jets with velocity ratios of 0, 0.2, 0.4 and 0.6 are shown in Fig. 7. For the jets with $U_L/U_U \leq 0.2$, there are two dominant frequencies in the spectra, one at $fH_j/U_a \approx 0.2$ near the jet exit corresponding to the large scale structures in the inner shear layer of the upper jet and the other at $fH_j/U_a \leq 0.06$ after the jet attached to the wall corresponding to the structures in the wall jet. There was also evidence for low frequency oscillations near the jet exit similar to those observed in backward facing step[11] that are thought to be associated with the flapping of the recirculating flow region.

In the jets with $U_L/U_U \geq 0.4$, there is another prominent frequency at $fH_j/U_a \approx 0.42$ in the spectra. This corresponds to a nondimensional frequency of $fH_c/U_a \approx 0.24$, when the frequency was normalized using the splitter plate thickness, $H_c$. A similar nondimensional frequency was found when the jet with a splitter thickness of 3.1cm was measured suggesting these motions are related to the wake downstream of the splitter plate. These motions had a narrow frequency band indicating they are initially highly periodic but they gradually diminished as the flow evolved downstream. A further discussion of these structures can be found in Gao and Ewing.[7]

The measurements suggest the lower jet initially develops like a wall jet flow when the velocity ratio is greater than approximate 0.4. This can be examined further by comparing the heat transfer coefficients of the dual jets normalized using the lower jet velocity and length scale of the lower jet. The resulting Stanton numbers are shown in Fig. 8 with results determined for a planar wall jet exiting the lower jet (with no flow out of the upper jet). The results showed that the Stanton number for all the jets decreased near the exit, $x/H_j \leq 2$, similar to the planar wall jets. The Stanton number for jet with velocity ratio of 0.8 agreed with the planar wall jet with similar Reynolds number up to $x/H_j \approx 6$. For lower velocity ratios, the Stanton number increased downstream of the exit due to the affect of the outer shear layer.

The skin friction and Stanton number for the different cases are compared in Fig. 9. The skin friction for

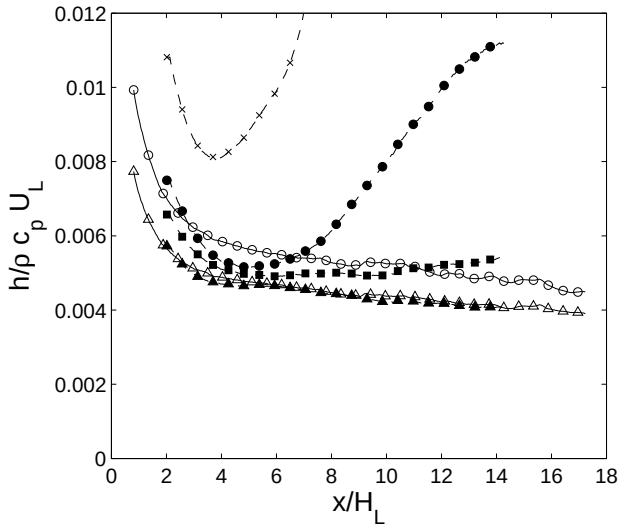


**Figure 8. Distributions of Stanton number for jets with a upper jet velocity of $U_U \approx 18.0$m/s and $U_L/U_U \approx$ × 0.2, • 0.4, ■ 0.6, ▲ 0.8 and planar wall jets with a Reynolds number of $U_L H_L/\nu =$ ○ 9400 and △ 16000.**

a planar wall jet was also shown in this figure. The skin friction for jets with $U_L/U_U \leq 0.2$ became similar to planar wall jet downstream of the reattachment location. This occurred quite rapidly for the offset jet, but took longer distance when the lower jet velocity was present. For jets with $U_L/U_U \geq 0.4$, the skin friction approached the skin friction for planar wall jet in the region examined here. The Stanton number for the jets with $U_L/U_U \leq 0.2$ did not decreased in the region $x/H_j \approx 9$ because of the interaction of the outer shear layer with the wall. The Stanton number for all the jets then decreased gradually downstream of this region and were similar in the region $x/H_j \geq 14$.

## IV. Concluding Remarks

The development of offset attaching planar jets with co-flowing jets was studied experimentally to examine the effect of the velocity ratio on the development of the jet. The experiments were performed for the case when the height of the lower jet was approximately half the upper jet and the offset distance of the upper jet was equal to the upper jet height. The results showed that the lower co-flowing jet separated from the wall and was entrained by the upper jet when the lower velocity was less than approximately $0.3U_U$. The resulting jet reattached further from the jet exit as the lower jet velocity increased, while the static pressure and the skin friction decreased in the recirculation region. The Stanton number and the fluctuating wall pressure both reached a maximum near the attachment location, and these maxima decreased when the lower jet velocity increased. The Stanton number in this impingement region was associated with the velocity of the reattaching flow and the turbulence, while the skin friction coefficient seemed to be more closely related to static pressure gradient.

When the lower jet velocity was $0.4U_U$ or higher, the two jets begin to develop parallel to each other causing the formation of a wake behind the splitter plate. There was no evidence of a mean separation near the wall and the skin friction and the heat transfer were initially similar to planar wall jet. The formation of the wake region behind the splitter plate dramatically increased the vertical component of the fluctuating velocity, $v'$, and the Reynolds stress, $\langle uv \rangle$, in the inner shear layer of the outer jet. The skin friction and the heat transfer in the region where the outer jet interacted with the wall were significantly lower than in the offset jets despite the large increase in the turbulence. In these cases, the skin friction and heat transfer near the jet outlet were determined by the wall jet flow created by the lower jet. The heat transfer and skin friction approached that for the offset jet from below. In these cases, the momentum transfer from the outer jet to the wall seem to be driven by the turbulent transport process across the jet, rather than the process associated with the shear layer impinging on the surface.

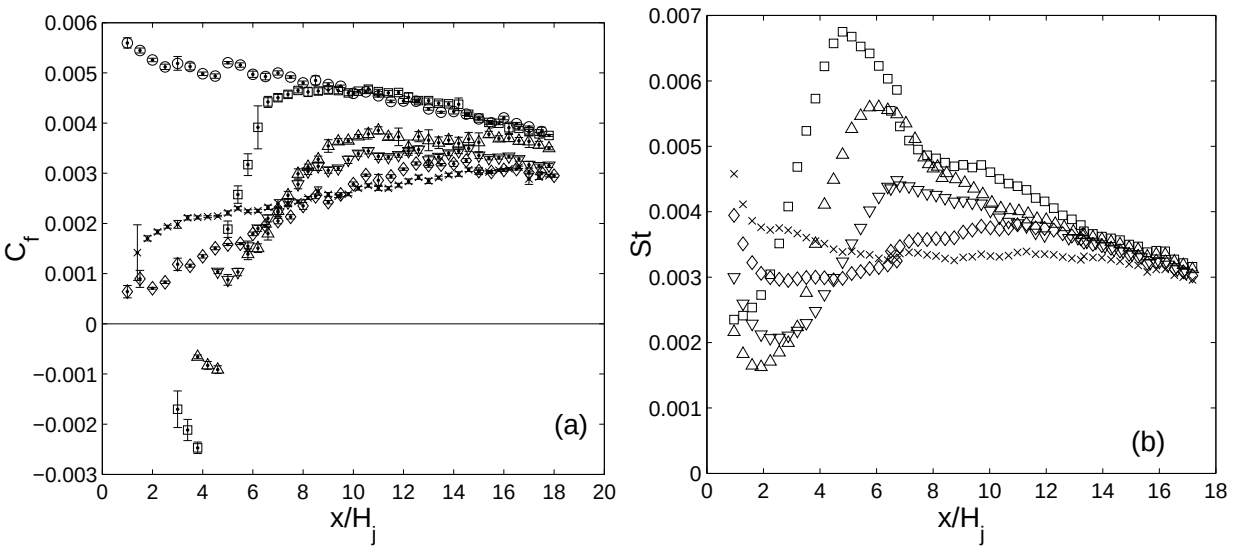


**Figure 9. Distributions of the (a) skin friction coefficient and (b) Stanton number for ○ a planar wall jet and jets with velocity ratio of $U_L/U_U$ = □ 0, △ 0.2, ▽ 0.4, ◇ 0.6, and × 0.8.**

## V. Acknowledgement

The research was funded by Natural Sciences and Engineering Research Council of Canada.

## References

[1]Beuther, P.D., "Experimental investigation of the axisymmetric turbulent buoyant plume", Ph.D. Thesis, The State University of New York at Buffalo, 1980

[2]Bradshaw, P. and Wong, F.Y.F., "The reattachment and relaxation of a turbulent shear layer", J. Fluid Mech., 52, pp.113-35, 1972

[3]Bruun, H.H., "Hot-wire Anemometry", Oxford University Press, Oxford, 1995

[4]Coleman, H. W. and Steele, W. G., "Experimentation and uncertainty analysis for engineers, 2nd edition, John Wiley & Sons., NY, 1999.

[5]Forliti, D.J. and Strykowski, P.J., "Controlling turbulence in a rearward-facing step combustor using countercurrent shear", ASME J. Fluids Engineering, 127, pp.438-448, 2005

[6]Gao, N. and Ewing, D., "Investigation of the large-scale flow strucutres in the cooling jets used in the blown film manufacturing process",ASME J. Fluids Engineering, 127, pp.978-985, 2005

[7]Gao, N. and Ewing, D., "Investigation of the large scale flow structures in dual planar attaching jets", AIAA paper 2006-0313

[8]Gao, N., Li, S. and Ewing, D., "Investigation of cooling jets used in blown film manufacturing process", Int. Polym. Proc., 20, pp.68-77, 2005

[9]Gao, N., Sun, H. and Ewing, D., "Heat transfer to impinging round jets with triangular tabs", Int. J. Heat Mass Transfer, 46, pp.2557-2569, 2003

[10]George W. K., Beuther P. D., Shabbir A., "Polynomial Calibrations for hot wires in thermally varying flows" Expt. Thermal Fluid Sci. 2, pp. 230–235, 1989.

[11]Heenan, A.F. and Morrison, J.F., "Passive control of pressure fluctuations generated by separated flow", AIAA J., 36, pp.1014-1022, 1998

[12]Jovic, S. and Driver, D. M., "Reynolds number effects on the skin friction in separated flows behind a backward facing step". Exps. Fluids, 18, pp.464-467, 1995

[13]Lund, T., "Augmented thrust and mass flow associated with two-dimensional jet reattachment", AIAA J., 24, pp1964-1970, 1986

[14]Nasr, A. and Lai, J., "A turbulent plane offset jet with small offset ratio", Experiments in Fluids, 24, pp.47-57, 1998

[15]Kim, D., Yoon, S., Lee, D. and Kim, K., "Flow and heat transfer measurements of a wall attaching offset jet", Int. J. Heat Mass Transfer, 39, pp.2907-2913, 1996

[16]Naughton, J.W. and Sheplak, M., "Modern developments in shear-stress measurement", Progress in Aerospace Sciences, 38, pp.515-570, 2002

[17]Naughton, J.W., Viken, S., and Greenblatt, D., "Skin Friction Measurements on the NASA Hump Model", accepted for publication in AIAA Journal, 2006

[18]Sawyer, R. A., "The flow due to a two-dimensional jet issuing parallel to a flow plate", J. Fluid Mech., 9, pp.543-560, 1960

[19]Sawyer, R. A., "Two-dimensional reattachment jet flows including the effect of curvature on entrainment", J. Fluid Mech., 17, pp.481-498, 1963

[20]Tanaka, T., Tanaka, E. and Nagai, K., "Study on control of radial attaching jet flow (1st report, effect of control flow on main jet flow near a nozzle)", Bulletin of JSME, 29, pp.1135-1140,1986

[21]Tanaka, T., Tanaka, E. and Nagaya, S., "Study on control of radial attaching jet flow (2nd report, effect of control flow on pressure distributions)", Bulletin of JSME, 29, pp.2049-2054,1986

[22]Tanaka, T., Tanaka, E. and Inque, Y., "Study on control of radial attaching jet flow (3rd report, flow before reattachment point)", Bulletin of JSME, 29, pp. 2482-2486, 1986

[23]Vogel, J.C. and Eaton, J.K., "Combined heat transfer and fluid dynamic measurements downstream of a backward-facing step", ASME J. Heat Transfer, 107, pp.922-929, 1985